Pilot-Free Data Detection in Uplink Cell-Free Massive MIMO Communication Systems

N V Divya Lakshmi, Arun Deshwal, and Adarsh Patel
School of Computing and Electrical Engineering (SCEE), Indian Institute of Technology Mandi, Mandi, India
Email: S22007@students.iitmandi.ac.in, S19027@students.iitmandi.ac.in, adarsh@iitmandi.ac.in

***Abstract*—In cell-free massive multiple-input multiple-output (CF-mMIMO) systems, a large number of distributed access points (APs) jointly serve users, eliminating traditional cell boundaries and enabling uniform coverage with high macro-diversity gains. However, the distributed topology and dense user–AP connectivity in coherent multiple-access-channel (MAC) make channel estimation significantly more challenging than in cellular systems, as conventional pilot-based methods incur excessive overhead and require tight inter-AP coordination. Addressing these limitations, a novel semi-blind detection (SBD) algorithm is proposed that models the received signal as a third-order tensor and jointly performs channel estimation and data detection without using the pilot transmission. Further, a lower computational complexity constrained semi-blind detection (CSBD) algorithm is presented for scenarios with known large-scale fading coefficients. Simulation results unequivocally demonstrate superior bit error rate (BER) performance of the proposed SBD and CSBD algorithms compared to iterative and pilot-assisted methods, instilling confidence in the robustness of presented algorithms.**

***Index Terms*—cell-free massive MIMO, semi-blind detection, joint channel estimation and data detection, tensor decomposition, and alternating least squares (ALS), modulation**

I. Introduction

As wireless communication networks progress towards 6G, the requirement for ubiquitous coverage, uniform Quality of Service, and high energy efficiency has become increasingly critical [1]. Cell-free massive multiple-input multiple-output (CF-mMIMO) is a promising solution that addresses these goals by combining the strengths of distributed antenna systems and massive MIMO technology [2]. Unlike conventional cellular networks, CF-mMIMO eliminates the notion of cells by deploying a large number of distributed access points (APs) that cooperatively serve all users [3]. This reduces the average distance between users and APs, thereby improving the overall system performance [4], [5].

Despite the aforementioned benefits, CF-mMIMO systems encounter significant obstacles in the domains of uplink channel estimation and data detection. The joint service of multiple users by each AP results in a network characterized by an extensive array of AP-user links, necessitating substantial training resources for accurate channel estimation. Additionally, when the number of users surpasses the available orthogonal pilot sequences, pilot contamination becomes an unavoidable issue, consequently serving as a critical performance bottleneck [6]. Although extending the pilot length can enhance the precision of estimation, it concurrently diminishes spectral efficie ncy, as it allocates a greater portion of resources to training rather than to data transmission [7]. In the context of centralized processing, the transmission of received signals from APs to the central processing unit (CPU) demands considerable fronthaul capacity and energy, a requirement that is particularly pronounced in densely deployed scenarios [8]. These challenges underscore the inherent trade-off between estimation accuracy and pilot overhead in conventional pilot-based detection schemes.

The application of *semi-blind* techniques has emerged as a potential solution to mitigate these challenges. In this context, *semi-blind* methods, employing restricted resources as opposed to extended ones, pertain to approaches that conduct channel estimation and subsequently followed by data detection [9]. This approach is particularly well-suited for CF-mMIMO, as it has the potential to mitigates pilot contamination, lowers fronthaul load and improves spectral efficiency, all critical for scalable and energy-efficient deployments. Some of these methods adopt distributed or decentralized architectures [10], [11], where each AP processes its local observations and exchanges soft information with neighboring APs or a central processor. While this reduces computational load on the CPU, it requires continuous information exchange and fronthaul coordination. Other approaches exploit inherent channel properties, e.g. sparsity [12]; or data properties, e.g. constellation hierarchy [13]; to simplify processing. Several methods also assume perfect knowledge of large-scale fading coefficients at the CPU [14], [15]. In spite of the progressive developments in the aforementioned methodologies, the integration of pilot symbols remains a critical necessity for the detection of data, thus contributing to the cumulative system overhead.

In a related domain of study, Parallel Factor Analysis (PARAFAC) leverages the inherent multi-dimensional structure of the received signal to distinctly identify its constituent factor matrices. This decomposition paradigm facilitates both blind and semi-blind detection methodologies. Blind detection recovers data without prior knowledge of factor matrices, while semi-blind detection uses one known matrix to aid recovery. The efficacy of PARAFAC in the context of signal separation is elaborated in [16] and has been empirically validated in MIMO [17], massive MIMO [18], and non-antipodal signaling based CF-mMIMO systems [19]. These findings underscore its capability for data recovery independent of explicit channel information.

However, despite these advances, tensor-based receivers

remain largely unexplored in the context of CF-mMIMO systems, for pilot-free joint channel estimation and data detection in large-scale wireless networks. Hence, the main contributions of this work are summarized below

- This work proposes a semi-blind data detection (SBD) algorithm that does not require pilot symbol transmission for channel estimation in coherent-MAC based CF-mMIMO networks. SBD is least-squares optimal and does not require the knowledge of large-scale fading coefficients as well.
- A variant of SBD called constrained-SBD (CSBD) is also proposed that exploits channel hardening for known large-scale coefficients for data detection. CSBD achieves a significant reduction in runtime, demonstrating that complexity can be reduced without compromising performance.
- Simulation results demonstrate a comparable performance of the proposed SBD over the traditional detection techniques with pilot transmission. Also, CSBD achieves a faster run time while maintaining the same Bit Error Rate (BER) as SBD.

Notations: Scalars are denoted by italic letters e.g. a, B; vectors by boldface lowercase letters e.g., $\mathbf{a}$, $\mathbf{b}$; matrices by boldface uppercase letters e.g., $\mathbf{A}$, $\mathbf{B}$; and tensors by script letters e.g. $\mathcal{A}$, $\mathcal{B}$. The operators $(\cdot)^T$, $(\cdot)^H$, $(\cdot)^*$, $(\cdot)^{-1}$, $(\cdot)^\dagger$, $\circ$, $\odot$, $\star$ represent transpose, hermitian, conjugate, inverse, pseudo-inverse, outer product, Khatri-rao product, and hadamard product operations [20] respectively. $\mathbf{A}^{(i)}$ refers to the intermediate matrix at iteration i. The mode-1, mode-2 and mode-3 unfoldings of a third order tensor $\mathcal{A} \in \mathbb{R}^{I_1 \times I_2 \times I_3}$ are $\mathbf{A}_{(1)}$, $\mathbf{A}_{(2)}$, and $\mathbf{A}_{(3)}$, respectively.

Section II delineates the system model under analysis. Section III elucidates the pilot-free data detection SBD and CSBD. Section IV offers the simulation outcomes and encapsulates the principal insights. Section V encapsulates the conclusions of the study.

II. System model

Consider an uplink time-division duplex (TDD) CF-mMIMO system illustrated in Fig. 1, where a CPU is connected to R APs, serving U users, with $R \gg U$. Both APs and users are equipped with single antennas and are randomly deployed in a geographic area. All R APs serve U users using the same time-frequency resources, forming a coherent multiple-access channel (MAC) based CF-mMIMO system. The element g_{ru} of the channel vector $\mathbf{g}u = [g_{1u} \cdots g_{ru} \cdots g_{Ru}]^T \in \mathbb{C}^{R\times 1}$, a block-faded wireless channel integrating large-scale and small-scale fading phenomena, represents the channel between AP r and user u, modeled as

$$g_{ru} = \sqrt{\beta_{ru}} h_{ru}, \tag{1}$$

and follows a complex Normal distribution, i.e., $g_{ru} \sim \mathcal{CN}(0, \beta_{ru})$. Here, β_{ru} denotes the large-scale fading coefficient, which captures path loss and shadowing effects, and is assumed to remain constant over several coherence intervals [21]. The small-scale fading coefficients h_{ru}, for all $r \in \{1, \cdots, R\}$ and $u \in \{1, \cdots, U\}$ are modeled as independent and identically distributed (i.i.d.) complex Gaussian random variables, with $h_{ru} \sim \mathcal{CN}(0, 1)$, and are assumed to remain constant within a coherence interval.

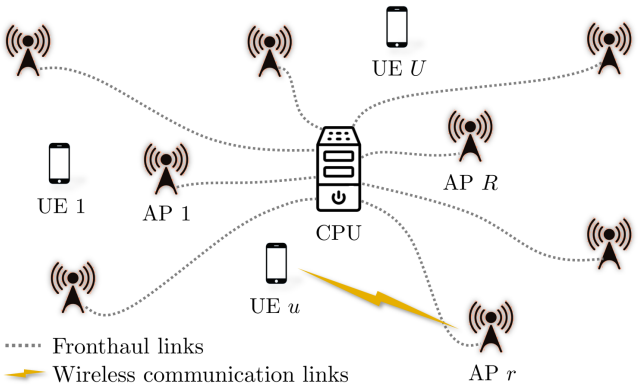

Fig. 1: A coherent multiple-access channel-based uplink Cell-free massive MIMO system with a central processing unit (CPU) connected to R single-antenna access points (APs) serving U single-antenna user equipments (UEs).

Let the data vector $\mathbf{d}_u \in \mathbb{R}^{K\times 1}$ of user u, be encoded by the corresponding code vector $\mathbf{s}_u \in \mathbb{R}^{L\times 1}$ as $\mathbf{d}_u \circ \mathbf{s}_u = \mathbf{d}_u \mathbf{s}_u^T \in \mathbb{R}^{K\times L}$, where the operator $\circ$ denotes the outer product [20]. The study considers inter-AP coordinated fronthaul links that are devoid of errors. The received signal $\mathbf{Y}_r \in \mathbb{C}^{K\times L}$ at AP r resulting from the transmission of the encoded data from all U users, is given by

$$\begin{aligned}\mathbf{Y}_r &= \sum_{u=1}^{U} \mathbf{d}_u \mathbf{s}_u^T g_{ru} + \mathbf{N}_r \\ &= \sum_{u=1}^{U} \mathbf{d}_u \circ \mathbf{s}_u \circ g_{ru} + \mathbf{N}_r,\end{aligned} \tag{2}$$

where $\mathbf{N}_r \in \mathbb{C}^{K\times L}$ is the noise matrix at AP r. Each element n_{kl} of $\mathbf{N_r}$ follows a complex normal distribution, i.e., $n_{kl} \sim \mathcal{CN}(0, \sigma_n^2)$. The received signal model in (2) can be equivalently expressed in matrix form as

$$\mathbf{Y}_r = \mathbf{D}\ \text{diag}\left([g_{r1} \ldots g_{ru} \ldots g_{rU}]\right) \mathbf{S}^T + \mathbf{N}_r, \tag{3}$$

where diag($\mathbf{a}$) is a diagonal matrix with the entries of vector $\mathbf{a}$ along its principal diagonal. Here, $\mathbf{D} = [\mathbf{d}_1 \ldots \mathbf{d}_u \ldots \mathbf{d}_U] \in \mathbb{R}^{K\times U}$ is the data matrix and $\mathbf{S} = [\mathbf{s}_1 \ldots \mathbf{s}_u \ldots \mathbf{s}_U] \in \mathbb{R}^{L\times U}$ is the code matrix. Each column u of $\mathbf{D}$ and $\mathbf{S}$ corresponds to the data vector $\mathbf{d}_u$ and the corresponding code vector $\mathbf{s}_u$ of user u. The received signals $\mathbf{Y}_r$, where $r \in \{1, \cdots, R\}$, defined in (3), are forwarded to the CPU for centralized processing. By stacking these matrices along mode-3, the composite received signal $\mathcal{Y} \in \mathbb{C}^{K\times L\times R}$ is obtained. Consequently, the received signal in the coherent MAC-based uplink CF-mMIMO system be represented as

$$\begin{aligned}\mathcal{Y} &= \sum_{u=1}^{U} \mathbf{d}_u \circ \mathbf{s}_u \circ \mathbf{g}_u + \mathcal{N} \\ &= \mathbf{D} \circ \mathbf{S} \circ \mathbf{G} + \mathcal{N},\end{aligned} \tag{4}$$

where the noise tensor $\mathcal{N} \in \mathbb{R}^{K\times L\times R}$ in (4) is obtained by stacking $\mathbf{N}_r \in \mathbb{C}^{K\times L}$ for $1 \leq r \leq R$ along mode-3 and the channel coefficient matrix $\mathbf{G}$ is defined as $\mathbf{G} = [\mathbf{g}_1 \dots \mathbf{g}_u \dots \mathbf{g}_U] \in \mathbb{C}^{R\times U}$, where $\mathbf{g}_u$ is given for (1). The received tensor $\mathcal{Y}$ at the CPU in (4) is represented as the sum of unit rank tensors, where the uth, $1 \leq u \leq U$, unit rank tensor $\mathbf{d}_u \circ \mathbf{s}_u \circ \mathbf{g}_u$ is obtained from the outer product of the uth column vectors of the corresponding matrices $\mathbf{D}, \mathbf{S}$ and $\mathbf{G}$ for $1 \leq u \leq U$. The next section develops a pilot-free detection framework, for the data matrix $\mathbf{D}$ in (4), in CF-mMIMO.

III. Pilot-free Data detection

The objective is to detect the transmitted signal $\mathbf{D}$ from the composite received signal tensor $\mathcal{Y}$ without pilot transmission in the uplink TDD CF-mMIMO system (4). The detection framework can be described as

$$\mathcal{L}(\hat{\mathbf{D}}, \hat{\mathbf{G}}) \triangleq \arg\min_{\mathbf{D},\mathbf{G}} \|\mathcal{Y} - \mathbf{D} \circ \mathbf{S} \circ \mathbf{G}\|_F^2, \tag{5}$$

where $\hat{\mathbf{D}}$ and $\hat{\mathbf{G}}$ are the reconstructed data and channel coefficient matrices, respectively, and $\mathbf{S}$ is the known code matrix. The cost function (5) is non-linear with unknown $\mathbf{D}$ and $\mathbf{G}$. Therefore, the task of reconstructing $\hat{\mathbf{D}}$ for an unknown $\hat{\mathbf{G}}$ presents a significant challenge. Alternating least squares (ALS) [22] solves the multi-objective cost function by alternately optimizing one factor matrix while keeping the others fixed. This converts the non-linear multi-objective cost function $\mathcal{L}(\hat{\mathbf{D}},\hat{\mathbf{G}})$ in (5) to its equivalent multiple linear least-square cost functions, described by $\mathcal{L}(\tilde{\mathbf{G}}^{(i)})$ and $\mathcal{L}(\tilde{\mathbf{D}}^{(i)})$ as

$$\mathcal{L}(\tilde{\mathbf{G}}^{(i)}) \triangleq \arg\min_{\mathbf{G}^{(i)}} \left\|\mathcal{Y} - \tilde{\mathbf{D}}^{(i-1)} \circ \mathbf{S} \circ \mathbf{G}^{(i)}\right\|_F^2 \tag{6}$$

$$\mathcal{L}(\tilde{\mathbf{D}}^{(i)}) \triangleq \arg\min_{\mathbf{D}^{(i)}} \left\|\mathcal{Y} - \mathbf{D}^{(i)} \circ \mathbf{S} \circ \tilde{\mathbf{G}}^{(i)}\right\|_F^2, \tag{7}$$

where $\mathbf{A}^{(i)}$ is the intermediate updated matrix at iteration $i \in \{1, \cdots, I\}$, with $\mathbf{A}^{(0)}$ denoting initialization. To solve (5), ALS alternately solves for $\tilde{\mathbf{G}}^{(i)}$ in (6) and $\tilde{\mathbf{D}}^{(i)}$ in (7) for a given $\tilde{\mathbf{D}}^{(i-1)}$ and $\tilde{\mathbf{G}}^{(i)}$, respectively. This process is repeated until convergence.

The mode-r unfolding or matricization of the tensor $\mathcal{X} \in \mathbb{R}^{J_1\times\cdots\times J_r\times\cdots\times J_N}$ of order N reshapes a tensor along mode-r into a matrix $\mathbf{X}_{(r)} \in \mathbb{R}^{J_r\times J}$ where $J = \Pi_{n=1,n\neq r}^{N} J_n$. Using the mode-$r$ marticization, the respective unfoldings of system model in (4) along mode-3 and mode-1 be defined as

$$\mathbf{Y}_{(3)} = \tilde{\mathbf{G}}^{(i)}(\mathbf{S} \odot \tilde{\mathbf{D}}^{(i-1)})^T + \mathbf{N}_{(3)} \tag{8}$$

$$\mathbf{Y}_{(1)} = \tilde{\mathbf{D}}^{(i)}(\tilde{\mathbf{G}}^{(i)} \odot \mathbf{S})^T + \mathbf{N}_{(1)}. \tag{9}$$

Thus $\mathbf{Y}_{(3)}$/$\mathbf{N}_{(3)}$ is mode-3 unfolding of tensor $\mathcal{Y}$/$\mathcal{N}$. Similarly, $\mathbf{Y}_{(1)}$/$\mathbf{N}_{(1)}$ corresponds to mode-1 unfolding of the tensor $\mathcal{Y}/\mathcal{N}$ and the operator $\odot$ denotes the Khatri-rao product [20]. The optimization problems in (6) and (7) when using the unfoldings of the received tensor $\mathcal{Y}$ in (8) and (9), are equivalently expressed as

$$\tilde{\mathbf{G}}^{(i)} = \arg\min_{\mathbf{G}^{(i)}} \left\|\mathbf{Y}_{(3)} - \mathbf{G}^{(i)}(\mathbf{S} \odot \tilde{\mathbf{D}}^{(i-1)})^T\right\|_F^2 \tag{10}$$

$$\tilde{\mathbf{D}}^{(i)} = \arg\min_{\mathbf{D}^{(i)}} \left\|\mathbf{Y}_{(1)} - \mathbf{D}^{(i)}(\tilde{\mathbf{G}}^{(i)} \odot \mathbf{S})^T\right\|_F^2. \tag{11}$$

The optimization problem in (10) and (11) are standard least squares problem with their respective solutions as

$$\tilde{\mathbf{G}}^{(i)} = \mathbf{Y}_{(3)}\left[(\mathbf{S} \odot \tilde{\mathbf{D}}^{(i-1)})^T\right]^\dagger \tag{12}$$

$$\tilde{\mathbf{D}}^{(i)} = \mathbf{Y}_{(1)}\left[(\tilde{\mathbf{G}}^{(i)} \odot \mathbf{S})^T\right]^\dagger, \tag{13}$$

where the operator $(\cdot)^\dagger$ denotes the Psuedo-Inverse [23]. The closed form expressions in (12) and (13) are solutions to the equivalent optimization problems in (10) and (11) at iteration i. The aim to solve for non-linear multi-objective cost function $\mathcal{L}(\hat{\mathbf{D}}, \hat{\mathbf{G}})$ in (5) is solved alternately/ iteratively solving for $\mathcal{L}(\tilde{\mathbf{G}}^{(i)})$ in (6) and $\mathcal{L}(\tilde{\mathbf{D}}^{(i)})$ in (7). The expressions in (12) and (13) are evaluated iteratively until a stopping criterion [22]. While the ALS approach provides an iterative framework for jointly updating the channel and data matrices, as shown in (12) and (13), it severely underperforms due to inherent permutation and scaling ambiguities of PARAFAC decomposition. To address the limitations identified, a pilot-free SBD algorithm predicated on the ALS method is introduced in the subsequent section.

Algorithm 1 Semi-Blind Detection (SBD) Algorithm

Input: $\mathcal{Y}, \mathbf{S}$

Initialize: $\hat{\mathbf{D}}^{(0)}$ with $\hat{\mathbf{D}}^{(0)}(1,:) = \mathbf{1}^T$

while $i < I$ and error $> \epsilon$ **do**
- $\tilde{\mathbf{G}}^{(i)} \leftarrow \mathbf{Y}_{(3)}[(\mathbf{S} \odot \hat{\mathbf{D}}^{(i-1)})^T]^\dagger$
- $\tilde{\mathbf{D}}^{(i)} \leftarrow \Re\{\mathbf{Y}_{(1)}[(\tilde{\mathbf{G}}^{(i)} \odot \mathbf{S})^T]^\dagger\}$
- $\mathbf{\Lambda}^{(i)} \leftarrow \text{diag}[\tilde{\mathbf{D}}^{(i)}(1,:)]$
- $\hat{\mathbf{D}}^{(i)} \leftarrow \tilde{\mathbf{D}}^{(i)}(\mathbf{\Lambda}^{(i)})^{-1}$
- $\hat{\mathbf{G}}^{(i)} \leftarrow \tilde{\mathbf{G}}^{(i)}\mathbf{\Lambda}^{(i)}$
- $\text{error}^{(i)} \leftarrow \|\mathbf{Y}_{(1)} - \hat{\mathbf{D}}^{(i)}(\hat{\mathbf{G}}^{(i)} \odot \mathbf{S})^T\|_F^2$
- $i \leftarrow i + 1$

end while

Output: $\hat{\mathbf{D}}, \hat{\mathbf{G}}$

A. Algorithm: Semi-Blind Detector (SBD)

This section outlines the proposed ALS-based SBD algorithm and explains how the permutation and scaling ambiguities are resolved using the known code matrix and simple post-processing steps. In this section, $\hat{\mathbf{A}}$ denotes the matrix with no ambiguity and $\tilde{\mathbf{A}}$ denotes it's counterpart with unresolved scaling ambiguity. *First*, the permutation ambiguity in PARAFAC, arising from arbitrary reordering of rank-one components, is resolved using the known structure of $\mathbf{S}$. Thereby ensuring the estimated channel and data vectors remain consistently ordered across iterations. Specifically, $\tilde{\mathbf{G}}^{(i)} = [\tilde{\mathbf{g}}_1^{(i)} \cdots \tilde{\mathbf{g}}_u^{(i)} \cdots \tilde{\mathbf{g}}_U^{(i)}]$, $\tilde{\mathbf{D}}^{(i)} = [\tilde{\mathbf{d}}_1^{(i)} \cdots \tilde{\mathbf{d}}_u^{(i)} \cdots \tilde{\mathbf{d}}_U^{(i)}]$, align with $\mathbf{S} = [\mathbf{s}_1 \cdots \mathbf{s}_u \cdots \mathbf{s}_U]$

for all $1 \leq u \leq U$, thus maintaining correct user-data association. *Second*, scaling ambiguity in PARAFAC involves arbitrary rescaling of rank-one components, with scaling in one factor offset by inverse scaling in another, preserving the overall tensor product. The SBD resolves scaling ambiguity by fixing the sign and magnitude of the first data bit of each user's BPSK signal, i.e., the matrix $\hat{\mathbf{D}}^{(0)}(1,:) = \mathbf{1}^T \in \mathbb{R}^{1\times U}$, providing a reference for all subsequent scaling corrections. During each iteration i, the algorithm alternates between updating the factor matrices $\tilde{\mathbf{G}}^{(i)}$ and $\tilde{\mathbf{D}}^{(i)}$ by fixing one matrix and solving for the other, as shown in Algorithm 1. This introduces diagonal scaling matrices $\mathbf{\Lambda}_D \in \mathbb{R}^{U\times U}$, $\mathbf{\Lambda}_G \in \mathbb{R}^{U\times U}$ which relate the estimated matrices $\hat{\mathbf{D}}^{(i)}$, $\hat{\mathbf{G}}^{(i)}$ to the matrices with ambiguities $\tilde{\mathbf{D}}^{(i)}$, $\tilde{\mathbf{G}}^{(i)}$ as

$$\tilde{\mathbf{D}}^{(i)} = \hat{\mathbf{D}}^{(i)}\mathbf{\Lambda}_D^{(i)}; \tilde{\mathbf{G}}^{(i)} = \hat{\mathbf{G}}^{(i)}\mathbf{\Lambda}_G^{(i)}; \text{ with } \mathbf{\Lambda}_D^{(i)}\mathbf{\Lambda}_G^{(i)} = \mathbf{I},$$

thus preserving the overall product. As $\mathbf{S}$ is known, any scaling induced in the columns of $\hat{\mathbf{D}}^{(i)}$ results in equal counter-scaling in columns of $\hat{\mathbf{G}}^{(i)}$, i.e., $\hat{\mathbf{D}}^{(i)} = \tilde{\mathbf{D}}^{(i)}[\mathbf{\Lambda}^{(i)}]^{-1}$ and $\hat{\mathbf{G}}^{(i)} = \tilde{\mathbf{G}}^{(i)}[\mathbf{\Lambda}^{(i)}]$ that results in $\hat{\mathbf{D}}^{(i)} \circ \mathbf{S} \circ \hat{\mathbf{G}}^{(i)} = \tilde{\mathbf{D}}^{(i)}(\mathbf{\Lambda}^{(i)})^{-1} \circ \mathbf{S} \circ \tilde{\mathbf{G}}^{(i)}\mathbf{\Lambda}^{(i)}$. The scaling diagonal matrix $\mathbf{\Lambda}^{(i)} = \text{diag}([\tilde{\mathbf{D}}^{(i)}(1,:)])$, where $\tilde{\mathbf{D}}^{(i)}(1,:)$ refers to the first row of $\tilde{\mathbf{D}}^{(i)}$. Convergence is monitored by computing the error metric

$$\text{error}^{(i)} = \|\mathbf{Y}_{(1)} - \hat{\mathbf{D}}^{(i)}(\hat{\mathbf{G}}^{(i)} \odot \mathbf{S})^T\|_F^2,$$

at each iteration using the ambiguity-corrected estimates. The iterative process continues until the error decreases below a predefined tolerance level ϵ, or the process is prematurely halted after reaching a specified number of iterations I. The final outputs $\hat{\mathbf{G}}$ and $\hat{\mathbf{D}}$ are free from scaling misalignment. The same steps are illustrated in Algorithm 1. It is important to acknowledge that, without compromising generality, the algorithm in question is equally applicable to higher-order modulation schemes. Furthermore, the detection performance is assessed utilizing the predefined stopping criteria. Building upon this foundational understanding, the subsequent section delves into the particular scenario wherein the large-scale fading coefficients are accessible at the CPU.

B. Constrained SBD (CSBD)

The updates for $\tilde{\mathbf{G}}^{(i)}$ and $\tilde{\mathbf{D}}^{(i)}$ in Algorithm 1 be modified for a known large-scale fading coefficients β_{ru}. Due to the inherent properties of channel hardening and favorable propagation in CF-mMIMO, the Gram matrix, i.e., $\tilde{\mathbf{G}}^{(i)H}\tilde{\mathbf{G}}^{(i)}$, becomes nearly diagonal as the number of APs increases, i.e., the channel norm $\|\mathbf{g}_u\|^2$ follows a hypoexponential distribution with mean $\sum_{r=1}^{R}\beta_{ru}$ and variance $\sum_{r=1}^{R}\beta_{ru}^2$. As R increases, the variance diminishes, and the Gram matrix can be approximated as a deterministic diagonal matrix $\mathfrak{D}_G = \text{diag}\left(\sum_{r=1}^{R}\beta_{r1}, \sum_{r=1}^{R}\beta_{r2}, \ldots, \sum_{r=1}^{R}\beta_{rU}\right)$. The known diagonal structure $\mathfrak{D}_G$ is exploited to simplify the data update $\tilde{\mathbf{D}}^{(i)}$ in Step 3 and the channel update $\tilde{\mathbf{G}}^{(i)}$ in Step 2 using Khatri-Rao product properties, eliminating the need to compute the pseudo-inverse of a dense matrix as

$$\begin{aligned}\left((\tilde{\mathbf{G}}^{(i)} \odot \mathbf{S})^T\right)^\dagger &= \left(\left(\tilde{\mathbf{G}}^{(i)H}\tilde{\mathbf{G}}^{(i)} * \mathbf{S}^H\mathbf{S}\right)^{-1}(\tilde{\mathbf{G}}^{(i)} \odot \mathbf{S})^H\right)^T \\ &= \left((\mathfrak{D}_G * L\mathbf{I}_U)^{-1}(\tilde{\mathbf{G}}^{(i)} \odot \mathbf{S})^H\right)^T,\end{aligned}$$

which leads to the following update steps in Algorithm 1

$$\tilde{\mathbf{G}}^{(i)} = \mathbf{Y}_{(3)}(\mathbf{S} \odot \tilde{\mathbf{D}}^{(i-1)})(L\,\text{diag}(\tilde{\mathbf{D}}^{(i-1)H}\tilde{\mathbf{D}}^{(i-1)}))^{-1} \quad (14)$$

$$\tilde{\mathbf{D}}^{(i)} = \Re\left\{\mathbf{Y}_{(1)}(\tilde{\mathbf{G}}^{(i)} \odot \mathbf{S})^*(L\,\mathfrak{D}_G)^{-1}\right\}. \quad (15)$$

CSBD converges faster than SBD, leveraging the known large-scale fading coefficients, which make the Gram matrix into a deterministic, real-valued diagonal matrix. The decrease in computational complexity from $\mathcal{O}(U^3)$ to $\mathcal{O}(U)$ is facilitated by the utilization of the known large-scale fading coefficient diagonal matrix [24], thereby achieving the same performance with a lower runtime.

IV. Simulation Results and Discussion

This section presents results which demonstrate the effectiveness of SBD and its variant, CSBD in uplink CF-mMIMO system with $R = 64$ APs and $U = 8$ users uniformly distributed in a $400\,\text{m}^2$ area. The data length $K = 16$, and code length $L = 16$. A wrap-around topology is used to mitigate edge effects. The large-scale fading is modeled as $\beta_{ru} = \min(1, d_{ru}^{-\alpha})$, where d_{ru} is the distance between user u and AP r, with $\alpha = 1$ [26]. The transmitted data matrix is partitioned as $\mathbf{D} = [\mathbf{D}_\text{p}^T\ \mathbf{D}_\text{d}^T]^T$, where $\mathbf{D}_\text{p} \in \mathbb{R}^{p\times U}$ contains pilot symbols and $\mathbf{D}_\text{d} \in \mathbb{R}^{(K-p)\times U}$ contains data symbols. The corresponding received signals and noise components are denoted as $\mathbf{Y}_{(3)} = [\mathbf{Y}_{(3),\text{p}}^T\ \mathbf{Y}_{(3),\text{d}}^T]^T$, and $\mathbf{N}_{(3)} = [\mathbf{N}_{(3),\text{p}}\ \mathbf{N}_{(3),\text{d}}]$, respectively (similarly for mode-1). Hence the received observations

$$\begin{aligned}\mathbf{Y}_{(3),\text{p}} &= \mathbf{G}(\mathbf{S} \odot \mathbf{D}_\text{p})^T + \mathbf{N}_{(3),\text{p}} \\ \mathbf{Y}_{(1),\text{d}} &= \mathbf{D}_\text{d}(\mathbf{G} \odot \mathbf{S})^T + \mathbf{N}_{(1),\text{d}}.\end{aligned}$$

The methodologies under comparison can be classified into two distinct categories:

1) Iterative methods: Namely, ALS, SBD, and CSBD, which perform joint channel estimation and data detection. The key distinctions lie in their initialization strategies, the way the factor matrices are updated, and how scaling ambiguity is resolved. The ALS method uses random initialization, and alternately updates the factor matrices using least squares (LS) solutions, without addressing the scaling ambiguity inherent in the problem. SBD improves upon this by introducing a strategic initialization by fixing the first row of the data matrix as $\hat{\mathbf{D}}^{(0)}(1,:) = \mathbf{1}^T$, which serves as a reference to eliminate the scaling ambiguity. The factor matrix is updated in the same manner as ALS. Building further, CSBD adopts the same initialization and ambiguity resolution mechanism as SBD, but simplifies the LS updates by exploiting the Khatri-Rao product properties. This allows the Gram matrix $\mathbf{G}^H\mathbf{G}$ to separate out, and be precomputed as $\mathfrak{D}_G$ at the CPU, derived from

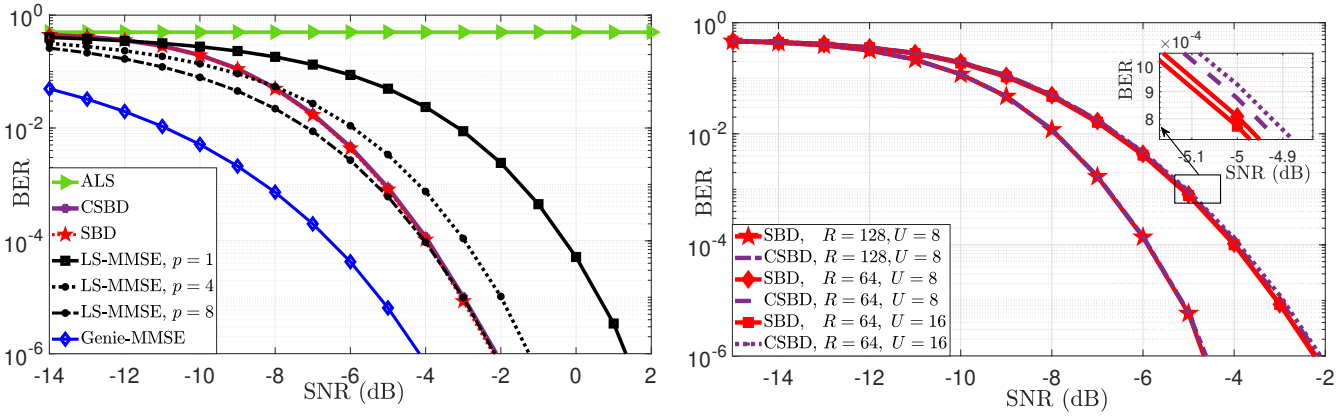

(a) (b)

Fig. 2: Performance of proposed SBD, CSBD in Section III-A for uplink CF-mMIMO with code length $L = 16$, (a) BER *vs.* SNR performance for $R = 64$ APs, and $U = 8$ users with ALS [22], pilot-assisted MMSE detection (LS-MMSE) [25] for $p \in \{1, 4, 8\}$ pilots, and perfect channel Genie-MMSE detection. (b) BER *vs.* SNR performance for users $U \in \{8, 16\}$ and APs $R \in \{64, 128\}$

the knowledge of large-scale fading coefficients. This avoids recomputing gram matrix in each iteration. All the iterative methods are truncated on reaching $I = 12$ iterations or when error reaches the tolerance $\epsilon = 10^{-4}$.

2) Baseline methods: Namely, pilot-assisted LS estimation followed by MMSE detection (LS-MMSE) and perfect CSI based Genie detection (Genie-MMSE). In the pilot-assisted case, for pilot lengths $p \in \{1, 4, 8\}$, LS channel estimation is performed as $\hat{\mathbf{G}}_{\text{LS}} = \mathbf{Y}_{(3),p} \left((\mathbf{S} \odot \mathbf{D}_p)^T \right)^{\dagger}$, followed by MMSE detection: $\hat{\mathbf{D}}_{\text{MMSE}} = \mathbf{Y}_{(1),d} \hat{\mathbf{G}}_{\text{LS}}^H \left(\hat{\mathbf{G}}_{\text{LS}} \hat{\mathbf{G}}_{\text{LS}}^H + \frac{1}{\text{SNR}} \mathbf{I} \right)^{-1}$. In the perfect CSI case, the channel $\mathbf{G}$ is assumed to be known, and MMSE detection is performed in the same way as in the pilot-assisted case, with $\hat{\mathbf{G}}_{\text{LS}} = \mathbf{G}$ in $\hat{\mathbf{D}}_{\text{MMSE}}$. The genie-aided setup thus serves as an ideal upper bound for performance and is used as a benchmark to evaluate all other methods. Note that all the techniques—both iterative and baseline—use the same pilot structure based on Hadamard sequences.

Fig. 2a compares the BER performance of ALS, SBD, CSBD, and pilot-assisted detection with $p \in \{1, 4, 8\}$, using Genie-MMSE as a benchmark. The results highlight three key insights. First, SBD and CSBD significantly outperform standard ALS, primarily due to strategic initialization and resolution of sign ambiguity, which standard ALS does not address. Second, SBD outperforms pilot-assisted detection despite using only a single pilot, whereas pilot-based methods require eight orthogonal pilots to achieve similar performance. Third, extensive experimentation confirms that the LS solution adopted in SBD is optimal. Therefore, the focus shifts to improving the efficiency of reaching this solution. This is effectively demonstrated by CSBD, which attains the same performance as SBD but with significantly lesser time.

Fig. 2b shows the BER performance of SBD and CSBD across different numbers of users $U \in \{8, 16\}$ and APs $R \in \{64, 128\}$, demonstrating the detectors' scalability. As R increases, BER improves due to enhanced spatial diversity. Notably, increasing U does not degrade performance, as each user contributes a distinct rank-1 tensor component that the proposed detectors effectively exploit. The performance of SBD and CSBD remains closely matched, with SBD achieving near-optimal solutions while CSBD attains comparable results more efficiently. Fig. 3 shows the maximum iterations versus average convergence time at SNR = -10dB. The CSBD converges faster than SBD while maintaining the same detection accuracy.

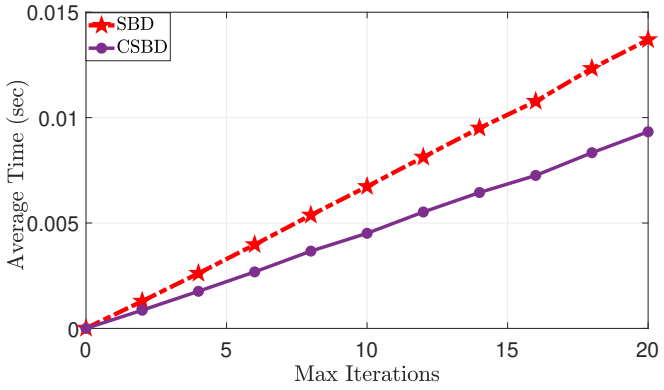

Fig. 3: Avg. run time *vs.* max. iterations at SNR = -10dB, $R = 64$ and $U = 8$.

V. Conclusion

The paper considered an uplink CF-mMIMO system and addressed the problem of data detection without sending the pilot signal. The problem is formulated within a tensor-based framework and solved using the proposed SBD, a data detection algorithm. The effectiveness of the proposed semi-blind detection method, SBD, uses only a single bit sign symbol, yet outperforms pilot-assisted MMSE detection, at high SNR, that relies on up to eight orthogonal pilots, demonstrating its effectiveness in low-overhead scenarios. A lower complexity constrained SBD algorithm is also presented for a known large-scale fading coefficients. The simulation results confirmed that the proposed SBD algorithm offers an optimal, robust, and scalable data detection.

REFERENCES

[1] International Telecommunication Union (ITU), "Recommendation ITU-R M.2160-0: Future technology trends of terrestrial IMT systems towards 2030 and beyond," Recommendation M.2160-0, ITU Radiocommunication Sector (ITU-R), 11 2023.

[2] Ö. T. Demir, E. Björnson, L. Sanguinetti, *et al.*, "Foundations of User-Centric Cell-Free Massive MIMO," *Foundations and Trends® in Signal Processing*, vol. 14, no. 3-4, pp. 162–472, 2021.

[3] H. Q. Ngo, A. Ashikhmin, H. Yang, E. G. Larsson, and T. L. Marzetta, "Cell-Free Massive MIMO Versus Small Cells," *IEEE Transactions on Wireless Communications*, vol. 16, no. 3, pp. 1834–1850, 2017.

[4] G. Interdonato, E. Björnson, H. Q. Ngo, P. Frenger, and E. G. Larsson, "Ubiquitous Cell-Free Massive MIMO Communications," *EURASIP Journal on Wireless Communications and Networking*, vol. 2019, p. 197, Aug. 2019.

[5] H. Yang and T. L. Marzetta, "Energy Efficiency of Massive MIMO: Cell-Free vs. Cellular," in *2018 IEEE 87th Vehicular Technology Conference (VTC Spring)*, pp. 1–5, 2018.

[6] T. L. Marzetta, "Noncooperative Cellular Wireless with Unlimited Numbers of Base Station Antennas," *IEEE Transactions on Wireless Communications*, vol. 9, no. 11, pp. 3590–3600, 2010.

[7] P. Liu, K. Luo, D. Chen, and T. Jiang, "Spectral Efficiency Analysis of Cell-Free Massive MIMO Systems With Zero-Forcing Detector," *IEEE Transactions on Wireless Communications*, vol. 19, no. 2, pp. 795–807, 2020.

[8] J. Zhang, S. Chen, Y. Lin, J. Zheng, B. Ai, and L. Hanzo, "Cell-Free Massive MIMO: A New Next-Generation Paradigm," *IEEE Access*, vol. 7, pp. 99878–99888, 2019.

[9] R. Gholami, L. Cottatellucci, and D. Slock, "Tackling Pilot Contamination in Cell-Free Massive MIMO by Joint Channel Estimation and Linear Multi-User Detection," in *2021 IEEE International Symposium on Information Theory (ISIT)*, pp. 2828–2833, 2021.

[10] A. Karataev, C. Forsch, and L. Cottatellucci, "Bilinear Expectation Propagation for Distributed Semi-Blind Joint Channel Estimation and Data Detection in Cell-Free Massive MIMO," *IEEE Open Journal of Signal Processing*, vol. 5, pp. 284–293, 2024.

[11] Z. Zhao and D. Slock, "Decentralized Message-Passing for Semi-Blind Channel Estimation in Cell-Free Systems Based on Bethe Free Energy Optimization," in *2024 58th Asilomar Conference on Signals, Systems, and Computers*, pp. 1443–1447, 2024.

[12] Z. Zhao and D. Slock, "Semi-Blind Sparse Channel Learning in Cell-Free Massive MIMO - a CRB analysis," in *ICC 2023 - IEEE International Conference on Communications*, pp. 5024–5029, 2023.

[13] Z. Zhao and D. Slock, "Hierarchical Expectation Propagation for Semi-Blind Channel Estimation in Cell-Free Networks," in *ICASSP 2025 - 2025 IEEE International Conference on Acoustics, Speech and Signal Processing (ICASSP)*, pp. 1–5, 2025.

[14] Z. Zhao and D. Slock, "Bilinear Hybrid Expectation Maximization and Expectation Propagation for Semi-Blind Channel Estimation," in *2024 32nd European Signal Processing Conference (EUSIPCO)*, pp. 2122–2126, 2024.

[15] Z. Zhao and D. Slock, "Expectation Propagation based Analysis of Semi-Blind Channel Estimation in Cell-Free Systems," in *2024 IEEE 25th International Workshop on Signal Processing Advances in Wireless Communications (SPAWC)*, pp. 836–840, 2024.

[16] A. L. F. de Almeida, G. Favier, J. P. C. L. Costa, and J. C. M. Mota, "Overview of Tensor Decompositions with Applications to Communications," in *Signals and Images: Advances and Results in Speech, Estimation, Compression, Recognition, Filtering, and Processing* (R. F. Coelho, V. H. Nascimento, R. L. de Queiroz, J. M. Romano, and C. C. Cavalcante, eds.), ch. 12, pp. 325–356, CRC-Press, Jan 2016.

[17] A. Deshwal and A. Patel, "Blind Distributed Detection in MIMO Networks," in *2024 16th International Conference on COMmunication Systems & NETworkS (COMSNETS)*, pp. 433–435, 2024.

[18] L. Zhao, S. Li, J. Zhang, and X. Mu, "A Parafac-Based Blind Channel Estimation and Symbol Detection Scheme for Massive MIMO Systems," in *2018 International Conference on Cyber-Enabled Distributed Computing and Knowledge Discovery (CyberC)*, pp. 350–3503, IEEE, 2018.

[19] N. V. D. Lakshmi and A. Patel, "Non–Antipodal Signaling–based Semi–Blind Detector in Uplink Cell–Free mMIMO Networks," in *2025 IEEE International Conference on Advanced Networks and Telecommunications Systems (ANTS)*, pp. 1–3, IEEE, 2025. Accepted, Nov 2025. Available: https://faculty.iitmandi.ac.in/~adarsh/Publications/Divya2025-ANTS-ERF-NonApSigBsdSemi-BlindDetCF-mMIMO.pdf.

[20] N. D. Sidiropoulos, L. De Lathauwer, X. Fu, K. Huang, E. E. Papalexakis, and C. Faloutsos, "Tensor Decomposition for Signal Processing and Machine Learning," *IEEE Transactions on Signal Processing*, vol. 65, no. 13, pp. 3551–3582, 2017.

[21] A. Ashikhmin, L. Li, and T. L. Marzetta, "Interference Reduction in Multi-Cell Massive MIMO Systems With Large-Scale Fading Precoding," *IEEE Transactions on Information Theory*, vol. 64, no. 9, pp. 6340–6361, 2018.

[22] T. G. Kolda and B. W. Bader, "Tensor Decompositions and Applications," *SIAM review*, vol. 51, no. 3, pp. 455–500, 2009.

[23] G. Strang, *Linear algebra and its applications*. Belmont, CA: Thomson, Brooks/Cole, 2006.

[24] N. D. Sidiropoulos, L. De Lathauwer, X. Fu, K. Huang, E. E. Papalexakis, and C. Faloutsos, "Tensor Decomposition for Signal Processing and Machine Learning," *IEEE Transactions on signal processing*, vol. 65, no. 13, pp. 3551–3582, 2017.

[25] S. Yang and L. Hanzo, "Fifty Years of MIMO Detection: The Road to Large-Scale MIMOs," *IEEE Communications Surveys & Tutorials*, vol. 17, no. 4, pp. 1941–1988, 2015.

[26] Z. Chen and E. Björnson, "Channel Hardening and Favorable Propagation in Cell-Free Massive MIMO with Stochastic Geometry," *IEEE Transactions on Communications*, vol. 66, no. 11, pp. 5205–5219, 2018.